Effect of Oxygen Plasma Treatment of Carbon Nanotubes on Electromagnetic Interference Shielding of Polypyrrole-Coated Carbon Nanotubes

Jumi Yun, Ji Sun Im, Hyung-Il Kim

Department of Fine Chemical Engineering and Applied Chemistry, BK21-E^{2}M, Chungnam National University, Daejeon 305-764, Republic of Korea

Received 30 September 2011; accepted 24 December 2011
DOI 10.1002/app.36709
Published online in Wiley Online Library (wileyonlinelibrary.com).

ABSTRACT: The polypyrrole (PPy)-coated multiwalled carbon nanotubes (MWCNTs) were prepared by *in situ* chemical oxidative polymerization of pyrrole on the surface of MWCNTs for the novel electromagnetic interference (EMI) shielding materials. The oxygen plasma treatment on MWCNTs introduced the hydrophilic functional groups resulting in uniform distribution of MWCNTs and higher interfacial affinity between PPy and MWCNTs. The uniform coating of PPy was formed on MWCNTs due to the effects of oxygen plasma treatment. The thermal stability of PPy-coated MWCNTs was improved by incorporation of MWCNTs. Absorption was the main mechanism of EMI shielding for the PPy-coated MWCNTs. The average EMI shielding efficiency of PPy-coated MWCNTs increased from 21.5 to 28.3 dB by oxygen plasma treatment of MWCNTs. © 2012 Wiley Periodicals, Inc. J Appl Polym Sci 000: 000–000, 2012

Key words: carbon nanotube; polypyrroles; oxygen plasma; electromagnetic interference

INTRODUCTION

The use of the electrical and electronics devices has been grown rapidly and it causes emitting of the electromagnetic energy in the same frequency bands with other electric devices resulting in the malfunction. As a result, it leads to the significant losses in time, energy, and resources. Electromagnetic interference (EMI) can also harm human bodies by causing diseases such as leukemia and breast cancer. Therefore, it becomes essential to limit and shield the electronic equipments against all sources of interference.[1–3]

Metals and metal oxides have usually been used as EMI shielding materials. However, they have disadvantages of not only cost and weight but also the secondary EMI from reflection. The application of polymers for housing of electronics device has many advantages due to light weight, flexibility, and relatively less cost. However, polymers are electrically insulating and transparent to electromagnetic radiation. Their inherent EMI shielding efficiency (SE) is practically zero. The incorporation of electrically conductive fillers in polymer matrices has been considered extensively to improve the EMI SE.[4–7]

The electrically conducting polymer-based composites were also investigated for EMI shielding applications. Polypyrrole (PPy) is one of the conducting polymers which have been studied extensively. PPy shows good conductivity, oxygen resistance, thermal and environmental stabilities, relative ease of synthesis, and innoxious characteristics, which are favorable for the various applications.[8,9] Carbon nanotubes (CNTs) have attracted interest as the electromagnetic wave-absorbing material among the electrically conductive fillers. CNTs possess high permittivity, which results in the high EMI SE. The high permittivity of CNTs is attributed to the well-organized carbon-graphite structure. The polymer composites containing a certain level of CNTs showed the electrical conductivity.[2,3,10–13] The interface affinity between polymer and hydrophobic CNTs plays an important role in the formation of polymer-based conducting composites.

Since the 1960s, plasma technology has quickly evolved into a valuable technique to engineer the surface properties without alteration of the bulk compositions.[14] Compared to other chemical modification methods, plasma treatment has the advantages of shorter reaction time, nonpolluting processing, and providing a wide range of functional groups depending on the plasma parameters. The plasma treatment is favored for the improvement in the interfacial affinity of composites because it modifies only the top few nm of the surface uniformly and it leaves the bulk properties of the material

Correspondence to: H.-I. Kim (hikim@cnu.ac.kr).

unchanged.[14,15] Oxygen plasma treatment provides the various polar functional groups such as C—O, C=O, O=C—O on the polymer surface, which alters the surface energy of materials and enhances the interfacial adhesion.[16–19]

In this study, the oxygen plasma treatment was employed to solve the poor dispersion and the lack of interfacial adhesion in the conducting polymer complex by introducing the functional groups on MWCNTs. A simple procedure of *in situ* chemical oxidative polymerization was carried out for the fabrication of PPy-coated MWCNTs. The effect of oxygen plasma treatment of MWCNTs on the EMI shielding behavior of PPy-coated MWCNTs was investigated in terms of permittivity, permeability, EMI SE, and EMI shielding mechanism.

EXPERIMENTAL

Materials

Pyrrole monomer (99%), ammonium persulfate (APS), and MWCNTs were purchased from Sigma–Aldrich. The diameter of MWCNTs was between 110 and 170 nm and the purity of MWCNTs was higher than 90%. Sodium dodecyl sulfate as surfactant was obtained from ICN Biomedicals. Hydrogen peroxide (H_2O_2) was purchased from Kanto Chemical.

Oxygen plasma treatment of MWCNTs

Plasma treatment was performed in a cylindrical discharge chamber. The system was pumped to a few Pascals by an oil rotary pump. Plasma was formed by an inductively coupled radio frequency generator, operating at a frequency of 13.56 MHz and a nominal power of about 100 W. Oxygen was introduced to the plasma instrument at the flow rate of 10 mL min^{-1}. The pressure was fixed at 200 mTorr. MWCNT samples were treated with oxygen plasma for various periods of time as 0, 5, 10, and 20 min and they were named hereafter as C0, C5, C10, and C20, respectively.

Synthesis of PPy-coated MWCNTs

PPy-coated MWCNTs were synthesized using *in situ* chemical oxidative polymerization on the oxygen plasma-treated MWCNT templates. The polymerization of pyrrole was carried out in the distilled water using H_2O_2 as oxidant and APS as initiator for pyrrole. A total of 0.3 g of oxygen plasma-treated MWCNTs was dispersed in the aqueous surfactant solution and ultrasonicated over 1 h. A total of 0.045 mol of pyrrole monomer was dropped into the MWCNTs dispersion slowly and the dispersion was stirred continuously for 10 min. Then, a total of 0.045 mol of H_2O_2 was added in the dispersion and a total of 0.8 g of APS dissolved in 10 mL distilled water was slowly added in the dispersion. The polymerization was carried out at 0°C for 6 h with constant mechanical stirring. The synthesized PPy-coated MWCNTs were filtered and rinsed several times with the distilled water, methanol, and acetone, respectively. PPy-coated MWCNTs were dried under vacuum at 40°C for 24 h. PPy-coated MWCNTs are classified as PC0, PC5, PC10, and PC20, respectively, depending on the time period of oxygen plasma treatment on MWCNTs.

Characterization

The X-ray photoelectron spectroscopy (XPS) spectra of oxygen plasma-treated MWCNTs were obtained with a MultiLab 2000 spectrometer (Thermo Scientific, England) to determine the chemical changes on the surface of MWCNTs caused by the oxygen plasma treatment. Al Kα (1485.6 eV) X-rays were used with a 14.9 keV anode voltage, a 4.6 A filament current, and a 20 mA emission current. All samples were treated at 10^{-9} mbar to remove impurities. The survey spectra were obtained with a 50 eV pass energy and a 0.5 eV step size. Core level spectra were obtained at a 20 eV pass energy with a 0.05 eV step size.

UV spectrometry (Optizen 2120 UV, Mecasys, Korea) was used to investigate the dispersion stability of oxygen plasma-treated MWCNTs in distilled water. The measurement was carried out following the general method presented by other groups.[20,21] UV transmittance was obtained as the average from five measurements at 635 nm after sonication for 1 h.

Field emission scanning electron microscopy (FE-SEM, S-5500, Hitachi, Japan) was used to investigate the surface morphology. Images were taken without prior treatment to ensure the acquisition of accurate images.

The functional groups of PPy, MWCNTs, and PPy-coated MWCNTs were investigated by Fourier transform infrared spectrometer (FT-IR, Nicolet, Magna IR550) to confirm the formation of PPy on the surface of MWCNTs.

Thermogravimetric analysis (TGA) was performed under air flow (25 cm^3 min^{-1}) at a heating rate of 10°C min^{-1} using Perkin Elmer TGA5OH thermogravimetric analyzer.

EMI SE measurement

Permittivity, magnetic permeability, and EMI SE were obtained according to the ASTM D-4935-99 method using a network analyzer (E5071A, Agilent Technologies, USA) equipped with an amplifier and a scattering parameter (*S*-parameter) test set over a frequency range of 800 MHz to 3 GHz.[22–24] Annular

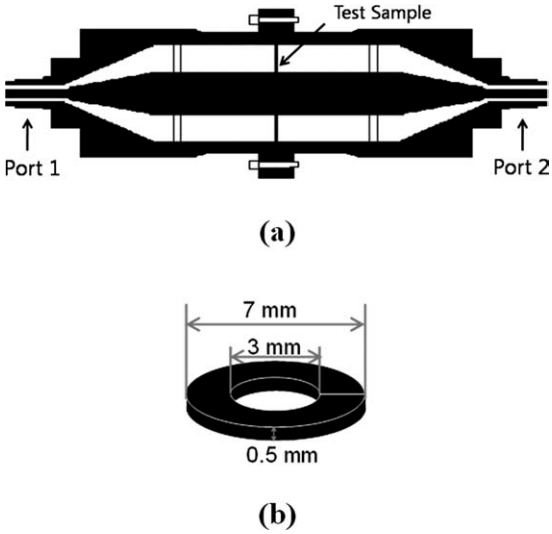

Scheme 1 Structure of the EMI SE holder (a) and the shape and dimensions of EMI SE test specimen (b).

disks were prepared with a punching machine and were installed into the test tool as shown in Scheme 1. The PPy-coated MWCNTs powders were pressed by a punching machine at 30 bar for getting a annular disk-typed sample. The detailed dimensions of a sample are presented in Scheme 1(b). EMI SE was calculated using *S* parameters with the use of equations found in the literatures.[22–24]

RESULTS AND DISCUSSION

Introduction of functional groups on MWCNTs by oxygen plasma treatment

The elemental survey data of the pristine and the oxygen plasma-treated MWCNTs are shown in Figure 1. The small O1s peak for the pristine MWCNTs represented the oxygen atoms from the partially oxidized MWCNTs in ambient atmosphere. Both C1s and O1s peak intensities varied depending on the treatment time of oxygen plasma.

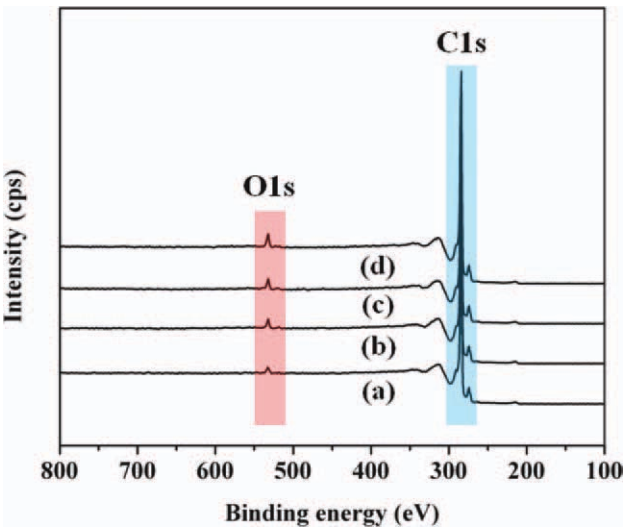

Figure 1 XPS spectra of various oxygen plasma-treated MWCNTs; (a) C0 (pristine), (b) C5, (c) C10, and (d) C20. [Color figure can be viewed in the online issue, which is available at wileyonlinelibrary.com.]

C1s peaks were deconvoluted to several pseudo-Vogit functions (sum of Gaussian–Lorentzian function) to investigate the chemical structures in detail using a peak analysis program obtained from Unipress, USA. The pseudo-Vogit function is given by[25]:

$$F(E) = H\left[(1-S)\exp\left(-\ln(2)\left(\frac{E-E_0}{\mathrm{FWHM}}\right)^2\right) + \frac{S}{1+\left(\frac{E-E_0}{\mathrm{FWHM}}\right)^2}\right] \quad (1)$$

where *F(E)* is the intensity at energy *E*, *H* is the peak height, E_0 is the peak center, FWHM is the full width at half maximum, and *S* is the shape function related to the symmetry and Gaussian–Lorentzian mixing ratio. The assignments of C1s components and the surface compositions of oxygen plasma-treated MWCNTs are listed in Table I. The details about C1s deconvolution were presented in our previous papers.[26,27]

Figure 2 shows the deconvoluted C1s peaks. C(1) peak corresponds to nonfunctionalized sp^2 carbon atoms which come from the aromatic carbons of MWCNTs.[28] The concentration of C(1) decreased from 90.3 to 73.5% by increasing the oxygen plasma treatment time. Oxygen reacted with the carbons in MWCNTs during plasma treatment resulting in the breakage of sp^2 carbon aromatic structure. C(2) and C(3) components were assigned to C—O and C=O, respectively. The intensities of these peaks increased by increasing the oxygen plasma treatment time. The total content of carbon-oxygen single and double bonds increased up to 10.5 and 8.6% for C20, respectively. These carbon-oxygen bonds contributed to the improvement in surface hydrophilicity of MWCNTs. O1s deconvolution data coincide well with C1s deconvolution results as shown in Figure 3 and Table II.

TABLE I
C1s Assignments and Surface Compositions of Oxygen Plasma-Treated MWCNTs

Component	Peak position (eV)	Pristine	C5	C10	C20
C(1), C—C	284.73	90.3	85.5	79.3	73.5
C(2), C—OH	286.55	9.7	11.4	11.1	10.5
C(3), C=O	287.90	0	2.2	5.7	8.6
C(4), COOH	289.26	0	0.9	3.9	7.5

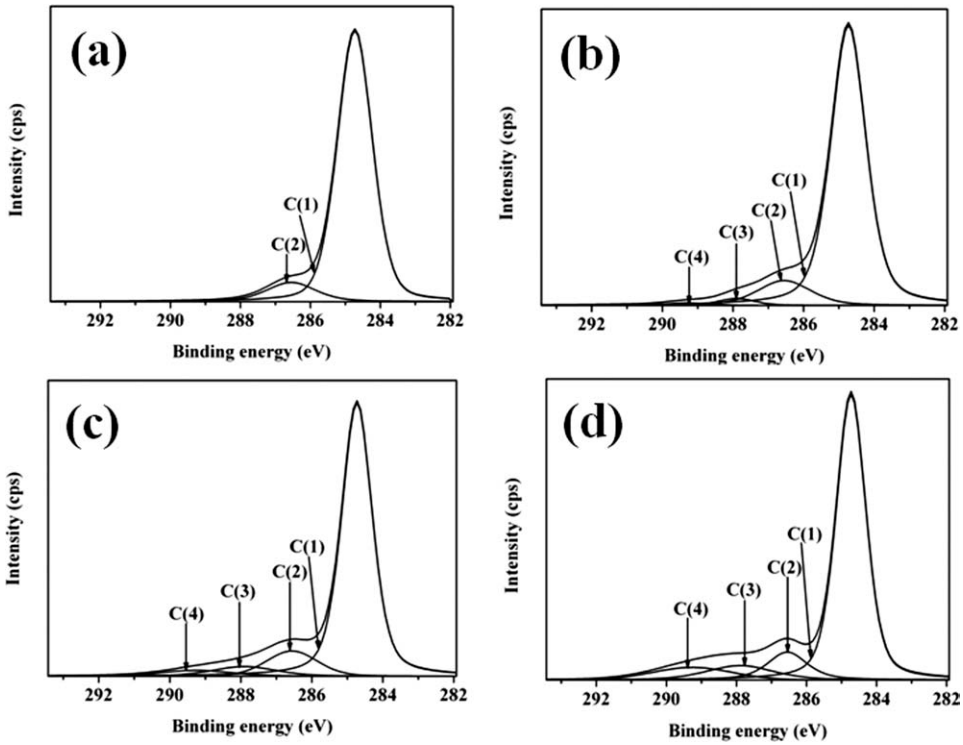

Figure 2 C1s deconvolution curves of various oxygen plasma-treated MWCNTs; (a) C0 (pristine), (b) C5, (c) C10, and (d) C20.

Improvement in dispersion stability of MWCNTs by oxygen plasma treatment

The dispersion stability of MWCNTs in aqueous media was investigated by measuring the transmittance variations depending on time as shown in Figure 4. The variation of UV transmittance of aqueous MWCNTs dispersion should be decreased for the highly stable MWCNTs dispersion because of less

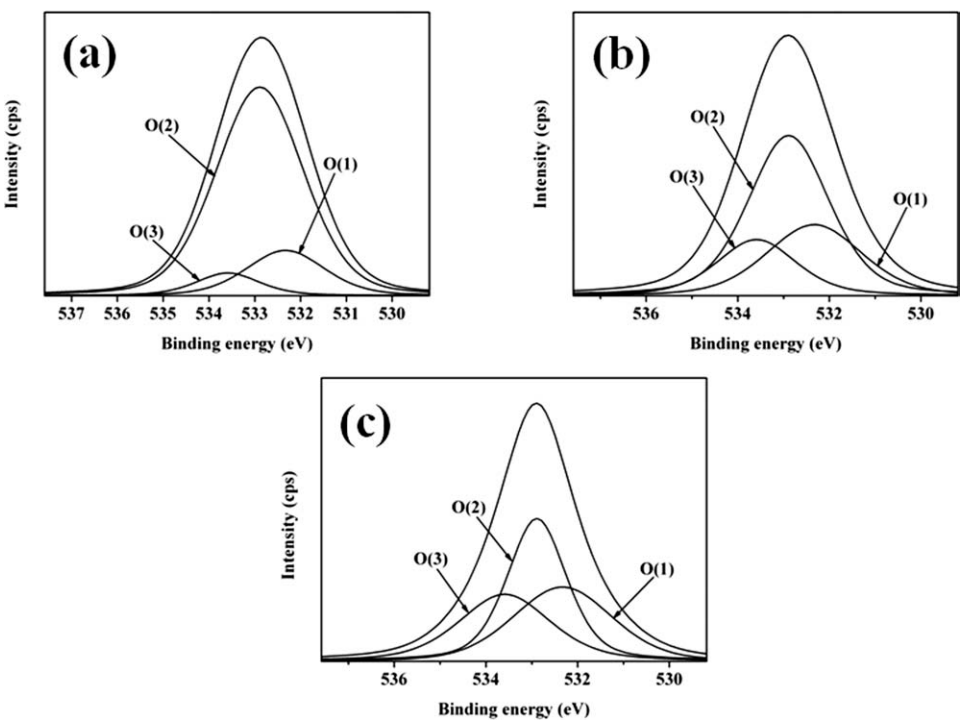

Figure 3 O1s deconvolution curves of various oxygen plasma-treated MWCNTs; (a) C5, (b) C10, and (c) C20.

TABLE II
O1s Assignments and Surface Compositions of Oxygen Plasma-Treated MWCNTs

Component	Peak position (eV)	C5	C10	C20
O(1), C=O	532.33	15.3	27.7	32.3
O(2), C—OH	532.89	78.5	53.5	39.4
O(3), COOH	533.59	6.1	18.8	28.3

coagulation of MWCNTs in aqueous media. Even though this method is an indirect method for evaluating the dispersion stability, it is widely used for the evaluation of dispersion stability due to the simple procedure and reasonable precision.[20,21] The transmittances of aqueous dispersions containing the pristine and the plasma-treated MWCNTs were measured at 635 nm. The improved stability of MWCNTs dispersion was confirmed by the lesser variations in transmittance. The dispersion stability of MWCNTs was improved by increasing the oxygen plasma treatment time because the hydrophilic functional groups formed on MWCNTs alleviated the coagulation of MWCNTs in aqueous media effectively. The improved dispersion stability of MWCNTs is very beneficial for uniform coating of PPy on MWCNTs because polymerization of pyrrole on MWCNTs is carried out in aqueous dispersion condition.

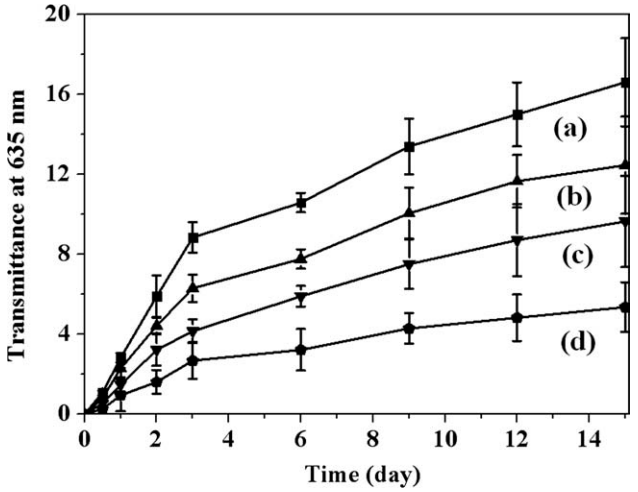

Figure 4 Dispersion stability of various oxygen plasma-treated MWCNTs; (a) C0 (pristine), (b) C5, (c) C10, and (d) C20.

Morphology variations of PPy-coated MWCNTs by oxygen plasma treatment

The morphologies of PPy-coated MWCNTs were investigated by SEM to investigate the effect of oxygen plasma treatment on MWCNTs as shown in Figure 5. PPy was coated uniformly on MWCNTs for both PC10 and PC20, in which MWCNTs were modified with oxygen plasma for a relatively long

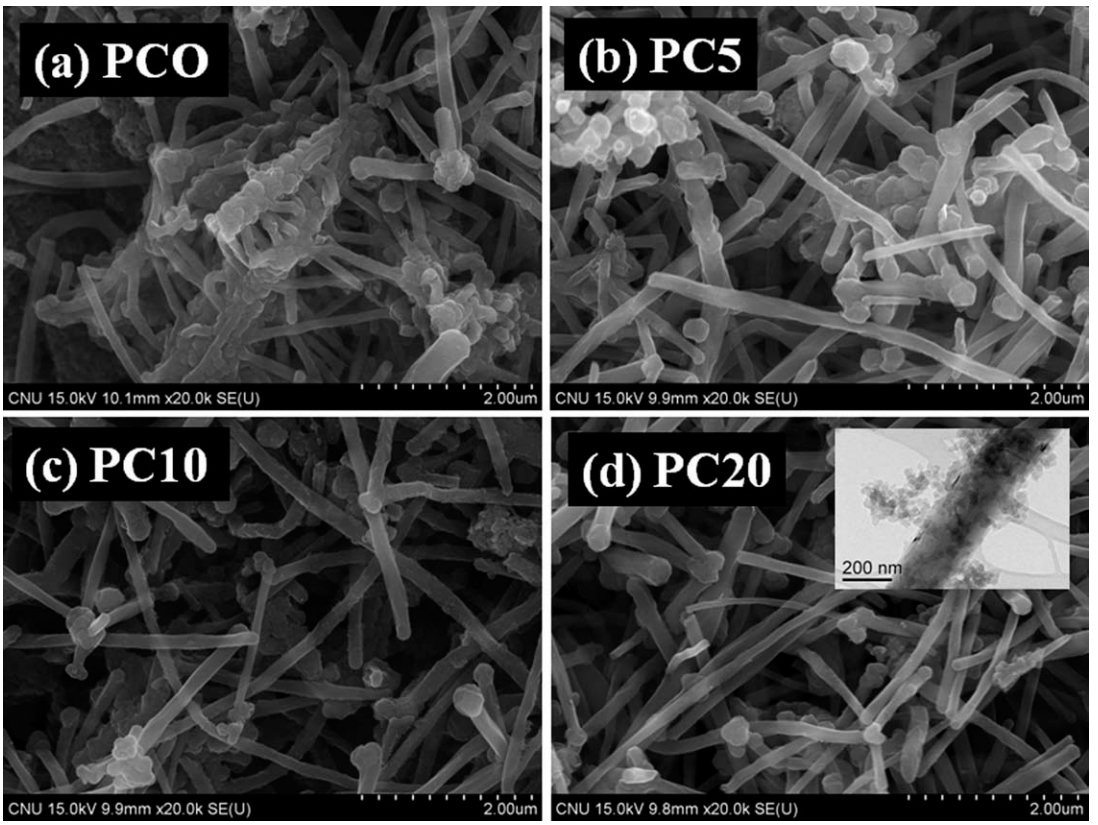

Figure 5 SEM micrographs of various PPy-coated MWCNTs. TEM micrograph of PC20 is inserted in (d).

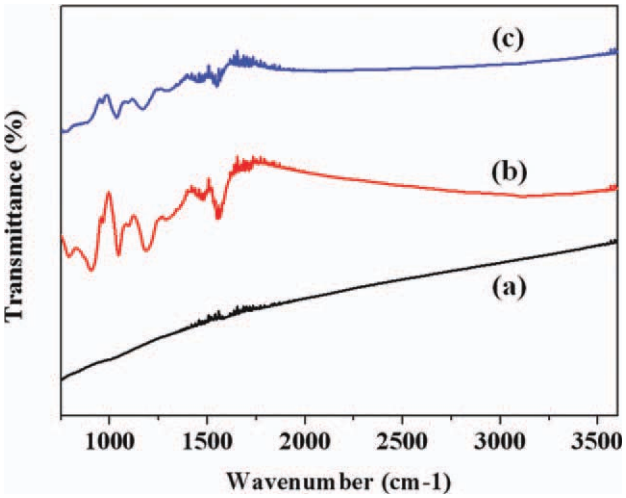

Figure 6 FT-IR spectra of (a) pristine MWCNTs, (b) PPy, and (c) PC20. [Color figure can be viewed in the online issue, which is available at wileyonlinelibrary.com.]

time. However, PC0 and PC5 samples showed the discrete PPy clusters of 200–400 nm in the space between MWCNTs instead of forming the PPy-coating on MWCNTs due to the poor interfacial affinity between PPy and the hydrophobic MWCNTs. The shorter exposure to the oxygen plasma was not enough to modify the surface of hydrophobic MWCNTs resulting in the ineffective template for the polymerization of pyrrole. The morphology of PPy-coated MWCNTs varied obviously depending on the oxygen plasma treatment time. The portion of segregated PPy clusters decreased noticeably and the more uniform coating of PPy on MWCNTs was produced by using more hydrophilically modified MWCNTs as in case of PC20 due to the improved interfacial affinity. This morphological feature was also confirmed by TEM images shown in the inserted picture of Figure 5(d).

FT-IR spectra of PPy-coated MWCNTs

The formation of polypyrrole on the surface of MWCNTs was confirmed by FT-IR spectra in Figure 6. There is no significant peak found in the pristine MWCNTs but the new peaks were observed at 1550, 3100–3130, and 3400–3410 cm^{-1} indicating the C=C, C—H, and N—H peaks, respectively, which were usually observed in PPy.[29,30] These peaks were also observed clearly in PPy-coated MWCNTs. This result supports the SEM images which showed the PPy formed on the surface of MWCNTs.

Thermal stability of PPy-coated MWCNTs

Thermal stability of PPy-coated MWCNTs was investigated by thermogravimetric analyzer as shown in Figure 7. MWCNTs are well known as the scavengers of free radicals.[31,32] Therefore, MWCNTs, which are dispersed uniformly in the polymer matrices, can retard the thermal decomposition of polymer effectively. Although PPy alone showed the poor thermal stability with initial decomposition stage around 100–250°C and secondary decomposition stage over 250°C, PPy-coated MWCNTs showed the obvious improvement in thermal stability due to the incorporation of MWCNTs. There was no noticeable difference found in thermal stability among various PPy-coated MWCNTs depending on the oxygen plasma treatment time. The MWCNTs contents in PPy-coated MWCNTs were measured from TGA data. The contents of MWCNTs were around 53 ± 2 wt % in all PPy-coated MWCNTs samples.

Permittivity and permeability of PPy-coated MWCNTs

Permittivity of PPy-coated MWCNTs is illustrated in Figure 8. The real permittivity was improved dramatically by introducing the hydrophilic functional groups on MWCNTs via oxygen plasma treatment. The real permittivity of sample is mainly associated with the polarization degree of the materials. Therefore, the polarization of PPy-coated MWCNTs seemed to increase due to the incorporation of hydrophilically modified MWCNTs. Compared with the permittivity of PC0, the permittivity of PC20 increased by ~ 70%. The imaginary permittivity also showed the similar trend as the real permittivity because the change of imaginary permittivity was strongly related to the change of real permittivity. The imaginary permittivity of PC20 increased about three times in comparison with that of PC0.

The permeability of PPy-coated MWCNTs is presented in Figure 9. The general trend of permeability

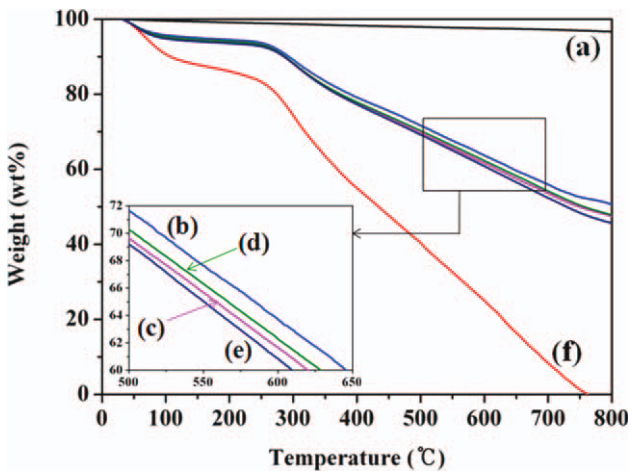

Figure 7 TGA thermograms of various PPy-coated MWCNTs; (a) C0 (pristine), (b) PC0, (c) PC5, (d) PC10, (e) PC20, and (f) PPy. [Color figure can be viewed in the online issue, which is available at wileyonlinelibrary.com.]

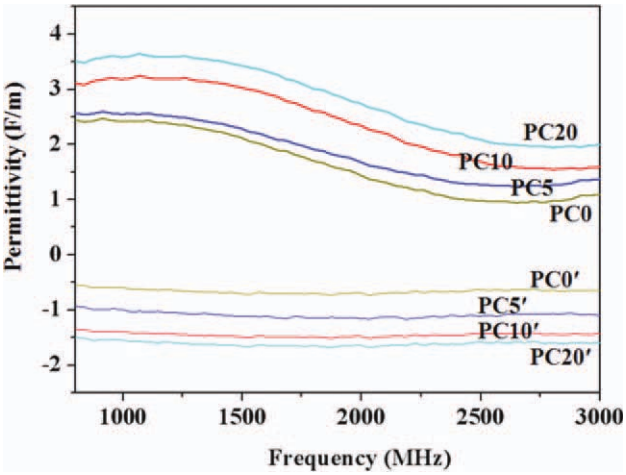

Figure 8 Permittivity of various PPy-coated MWCNTs. PC0, PC5, PC10, and PC20 represent the real permittivity and PC0′, PC5′, PC10′, and PC20′ represent the imaginary permittivity, respectively. [Color figure can be viewed in the online issue, which is available at wileyonlinelibrary.com.]

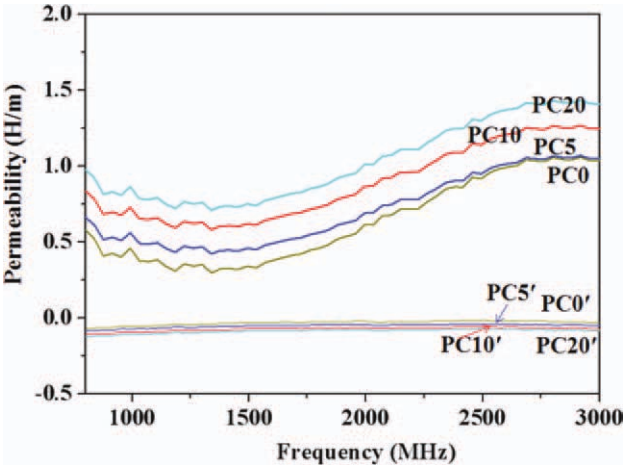

Figure 9 Permeability of various PPy-coated MWCNTs. PC0, PC5, PC10, and PC20 represent the real permeability and PC0′, PC5′, PC10′, and PC20′ represent the imaginary permeability, respectively. [Color figure can be viewed in the online issue, which is available at wileyonlinelibrary.com.]

variation was similar as permittivity behavior of PPy-coated MWCNTs. The real permeability of PC20 increased about 60% over that of PC0. The increased hydrophilic functional groups on MWCNTs were responsible for the improved permeability of PPy-coated MWCNTs samples. Therefore, PPy-coated MWCNTs containing the hydrophilically modified MWCNTs were effective as the EMI shielding materials. The improved permittivity and permeability of PPy-coated MWCNTs are mainly attributed to the electrical and magnetic properties of MWCNTs[33,34] and the surface treatment effects for the uniform distribution of MWCNTs as conductive templates.

EMI shielding efficiency of PPy-coated MWCNTs

EMI SE is a number that quantifies the amount of attenuation of electromagnetic wave. EMI SE can be expressed as:

$$\text{EMI SE} = 10\log(P_I/P_T) = 20\log|E_I/E_T| \quad (2)$$

where P_I (E_I) and P_T (E_T) are the power (electric field) of the incident and transmitted electromagnetic waves, respectively.[22–24]

Figure 10 shows the EMI SE of PPy-coated MWCNTs in the frequency range of 850–3000 MHz. The general trend in EMI SE of various PPy-coated MWCNTs looked similar as permittivity and permeability of those. EMI SE of PC20 increased around 40% over that of PC0. The hydrophilic functional groups on the surface of MWCNTs contributed to the improved interfacial affinity between PPy and MWCNTs for the formation of uniform distribution of MWCNTs in PPy matrices resulting in the higher EMI SE of PPy-coated MWCNTs. EMI SE decreased gradually at higher frequency ranges for all the samples due to the enhanced dielectric and magnetic losses in those frequency ranges.[35]

To investigate the contribution of both absorption and reflection to the total EMI SE of samples, *S* parameters were measured.[36] Transmittance (*T*), reflectance (*R*), and absorbance (*A*) coefficients were obtained using the *S* parameters.[37]

$$1 = A + R + T \quad (3)$$

$$T = |E_T/E_I|^2 = |S_{12}|^2 (= |S_{21}|^2) \quad (4)$$

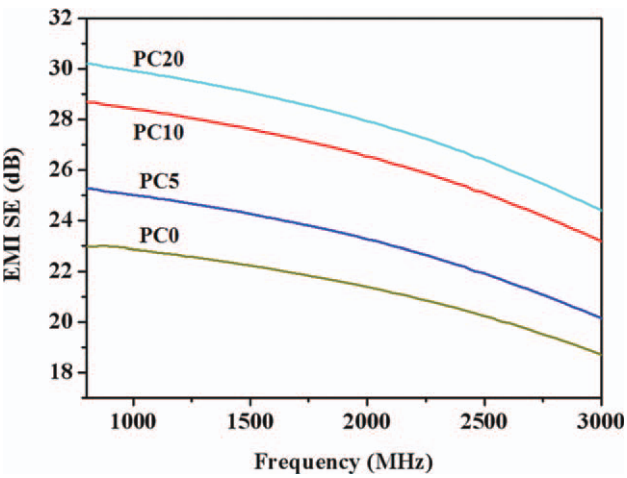

Figure 10 EMI SE of various PPy-coated MWCNTs. [Color figure can be viewed in the online issue, which is available at wileyonlinelibrary.com.]

$$R = |E_R/E_I|^2 = |S_{11}|^2 (= |S_{22}|^2) \quad (5)$$

In this study, the multiple reflection effects were not considered separately because the measured reflection power includes not only the power that has been reflected from the external surface but also the positive contribution from internal surface reflection and the negative contribution from multiple reflections.[38] As a result, shielding efficiencies by reflection (SE_R) and absorption (SE_A) were calculated by the following equations.[39,40]

$$SE_R = 10 \log \frac{I}{I - R} \quad (6)$$

$$SE_A = 10 \log \frac{I - R}{T} \quad (7)$$

$$SE = SE_R + SE_A = 10 \log \frac{I}{T} \quad (8)$$

Shielding efficiencies by absorption were calculated with above equations as 86, 89, 93, and 95% for PC0, PC5, PC10, and PC20, respectively. The shielding efficiency by absorption increased by incorporating the MWCNTs treated with oxygen plasma for longer time due to the excellent electrical conductivity of MWCNTs and the enhanced interfacial adhesion between MWCNTs and PPy matrices. The uniform coating of PPy on MWCNTs by controlling the surface properties also played a crucial role in increasing the electrical conductivity of PPy/MWCNT mixtures effectively resulting in the significant improvement of EMI SE.[41]

CONCLUSIONS

PPy-coated MWCNTs were prepared for the effective EMI shielding materials by *in situ* chemical oxidative polymerization. Hydrophilic functional groups formed on the surface of MWCNTs by oxygen plasma treatment were confirmed by XPS analysis. Hydrophilic functional groups on MWCNTs were responsible for the higher interfacial affinity between PPy and MWCNTs. The dispersion stability of MWCNTs in aqueous media was improved by oxygen plasma treatment. PPy could be uniformly coated on MWCNTs by increasing the oxygen plasma treatment time. The improved thermal stability of PPy-coated MWCNTs was confirmed by TGA analysis. The permittivity, permeability, and EMI SE of PPy-coated MWCNTs were significantly improved by introduction of hydrophilic functional groups on MWCNTs via oxygen plasma treatment. The average EMI SE of PPy-coated MWCNTs increased from 21.5 to 28.3 dB by incorporating the oxygen plasma-treated MWCNTs in PPy matrices.

References

1. Hung, F. S.; Hung, F. Y.; Chiang, C. M. Appl Surf Sci 2011, 257, 3733.
2. Li, Y.; Chen C. X.; Zhang, S.; Ni, Y.; Huang, J. Appl Surf Sci 2008, 254, 5766.
3. Kim, B. R.; Lee, H. K.; Park, S. H.; Kim, H. K. Thin Solid Films 2011, 519, 3492.
4. Arjmand, M.; Mahmoodi, M.; Gelves, G. A.; Park, S.; Sundararaj U.; Carbon 2011, 49, 3430.
5. Nam, I. W.; Lee, H. K.; Jang, J. H. Compos A Appl Sci Manuf 2011, 42, 1110.
6. Yun, J.; Im, J. S.; Lee, Y. S.; Kim, H. I. Eur Polym J 2010, 46, 900.
7. Kim, H. B.; Jeun, J. P.; Hong, S. M.; Kang, P. H. J Ind Eng Chem 2010, 16, 437.
8. Lu, Y.; Pich, A.; Adler, H. J. P.; Wang, G.; Rais, D.; Nešpůrek, S. Polymer 2008, 49, 5002.
9. Kaynak, A.; Rintoul, L.; George, G. A. Mater Res Bull 2000, 35, 813.
10. Zhang, C. S.; Ni, Q. Q.; Fu, S. Y.; Kurashiki, K. Compos Sci Technol 2007, 67, 2973.
11. Liu, Z.; Bai, G.; Huang, Y.; Ma, Y.; Du, F.; Li, F.; Guo, T.; Chen Y. Carbon 2007, 45, 821.
12. Kim, Y. Y.; Yun, J.; Lee, Y. S.; Kim, H. I. Carbon Lett 2011, 12, 48.
13. Zheming, G.; Chunzhong, L.; Gengchao, W.; Ling, Z.; Qilin, C.; Xiaohui, L.; Wendong, W.; Shilei, J. J Ind Eng Chem 2010, 16, 10.
14. Morand, S. Hattori, S. In Plasma Deposition, Treatment, and Etching of Polymers; d'Agostino, R., Ed.; Academic Press: Boston, 1990; p 423.
15. Canal, C.; Gaborian, F.; Villeger, S.; Cvelbar, U.; Ricard, A. Int J Pharm 2009, 367, 55.
16. Geyter, N.; Morent, R.; Leys, C.; Gengembre, L.; Payen, E. Surf Coat Technol 2007, 201, 7066.
17. Junkar, I.; Vesel, A.; Cvelbar, U.; Mozetič, M.; Strnad, S. Vacuum 2010, 84, 83.
18. Kim, Y. J.; Kang, I. K.; Huh, M. W.; Yoon, S. C. Biomaterials 2000, 21, 121.
19. Vesel, A.; Junkar, I.; Cvelbar, U.; Kovač, J.; Mozetič, M. Surf Interface Anal 2008, 40, 1444.
20. Park, O. K.; Jeevananda, T.; Kim, N. H.; Kim, S. I.; Lee, J. H. Script Mater 2009, 60, 551.
21. Arepalli, S.; Nikolaev, P.; Gorelik, O.; Hadjiev, V. G.; Holmes, W.; Files, B. Carbon 2004, 42, 1783.
22. Nicolson, A. M.; Ross, G. F. IEEE T Instrum Meas 1970, 19, 377.
23. Ghodgaonkar, D. K.; Vardan, V. V.; Varadan, V. K. IEEE T Instrum Meas 1990, 39, 387.
24. Hong, Y. K.; Lee, C. Y.; Jeong, C. K.; Lee, D. E.; Kim, K.; Joo, J. Rev Sci Instrum 2003, 74, 1098.
25. Wu, Z.; Li, J.; Timmer, D.; Lozano, K.; Bose, S. Int J Adhes Adhes 2009, 29, 488.
26. Yun, J.; Im, J. S.; Lee, Y. S.; Kim, H. I. Eur Polym J 2011, 47, 1893.
27. Im J. S.; Kim, J. G.; Bae, T. S.; Yu, H. R.; Lee, Y. S. Sens Actuators B Chem 2011, 158, 151.
28. Im J. S. Kang, S. C.; Bai, B. C.; Bae, T. S.; In, S. J.; Jeong, E.; Lee, S. H.; Lee, Y. S. Carbon 2011, 49, 2235.
29. Kate, H.; Nisbikawa, O.; Matsui, T.; Honma, S.; Kokado, H. J Phys Chem 1991, 95, 6014.
30. Davidson, R. G.; Turner, T. G. Synth Met 1995, 72, 121.
31. Kodjie, S. L.; Li, L.; Li, B.; Cai, W.; Li, C. Y.; Keating, M. J Macromol Sci B Phys 2006, 45, 231.
32. Im, J. S.; Bai, B. C.; Bae, T. S.; In, S. J.; Lee, Y. S. Mater Chem Phys 2011, 126, 685.

33. Zhang, C. S.; Ni, Q. Q.; Fu, S. Y.; Kurashiki, K. Compos Sci Technol 2007, 67, 2973.
34. Im, J. S.; Park, I. J.; In, S. J.; Kim, T.; Lee, Y. S. J Fluor Chem 2009, 130, 1111.
35. Im J. S.; Kim, J. G.; Lee, S. H.; Lee, Y. S. Mater Chem Phys 2010, 124, 434.
36. ASTM. American Society for Testing and Materials; ASTM: Philadelphia, PA, 1999; D-4935.
37. Ghodgaonkar, D. K.; Varadan, V. V.; Varadan, V. K. Trans Instrum Meas 1990, 39, 387.
38. Al-Saleh, M. H.; Sundararaj, U. Carbon 2009, 47, 1738.
39. Saini, P.; Choudhary, V.; Singh, B. P.; Mathur, R. B.; Dhawan, S. K. Mater Chem Phys 2009, 113, 919.
40. Hong, Y. K.; Lee, C. Y.; Jeong, C. K.; Sim, S. H.; Kim, K.; Joo, J.; Kim, M. S.; Lee, J. Y.; Jeong, S. H.; Byun, S. W. Curr Appl Phys 2001, 1, 439.
41. Yun, J.; Im, J. S.; Kim, H. I.; Lee, Y. S. Colloid Polym Sci 2011, 289, 1749.